Environmentally persistent free radicals mediated removal of Cr(VI) from highly saline water by corn straw biochars

Nan Zhao [a, b], Zheng Yin [a], Feng Liu [a], Meiyi Zhang [a], Yizhong Lv [c], Zhengping Hao [a, d], Gang Pan [a, e], Jing Zhang [a, d, *]

[a] *Department of Environmental Nano-materials, Research Center for Eco-Environmental Sciences, Chinese Academy of Sciences, Beijing 100085, China*

[b] *School of Environmental Science and Engineering, Guangdong Provincial Key Lab of Environmental Pollution Control and Remediation Technology, Sun Yat-sen University, Guangzhou, 510275, P.R. China*

[c] *College of Resources and Environmental Sciences, China Agricultural University, Beijing 100193, China*

[d] *National Engineering Laboratory for VOCs Pollution Control Materials & Technology, University of Chinese Academy of Sciences, Beijing 101408, P.R. China*

[e] *School of Animal, Rural and Environmental Sciences, Nottingham Trent University, Brackenhurst Campus, Nottinghamshire NG250QF, United Kingdom*

A B S T R A C T

Heavy metal ions coexisting with salts in the contaminant water are difficult to remove due to the interference of salts. Herein, biochars were pyrolyzed by corn straw at different temperatures, aiming to remove Cr(VI) in the presence of salts. Results show that biochars had surprisingly selective adsorption of Cr(VI). X-ray photoelectron and X-ray absorption near edge spectra revealed that Cr(VI) was reduced to Cr(III). All the adsorption was conducted at pH~7, which differed from the previous studies that Cr(VI) could only be reduced at pH 2~4. Environmental persistent free radicals (EPFRs) on biochars were found to play the role in reducing Cr(VI) in neutral solutions, which was confirmed by electron spin resonance and free radical quenching. The biochar with EPFRs reveals a highly selective removal of Cr(VI), which has implications for the remediation of contaminated water. This work

provides a new insight into biochar's properties and potential environmental applications.

Keywords: Corn straw biochar; Chromium; Environmental persistent free radicals; Selective adsorption; Reduction

1. Introduction

Heavy metal contamination of soil and water has received increasing concern because it can cause a severe threat to human health and ecosystems. Heavy metal ions are normally toxic, cumulative, and non-biodegradable. Among the most commonly presented heavy metals, hexavalent chromium, Cr(VI), released from textile dying, tanneries, electroplating, and metallurgical smelting of chromite ore, is highly diffusive and a well-known carcinogen. Many technologies have been applied to remove Cr(VI) from wastewater, including chemical reduction, ion exchange, ultrafiltration and so on (Ghosh and Bhattacharya, 2006; Mohan et al., 2006; Tiravanti et al., 1997; Yu et al., 2016). Adsorption is considered as a highly effective, relatively inexpensive, and easily handling method, where activated carbon, minerals, macromolecular polymers and nanomaterials are widely selected as adsorbents in the remediation of Cr(VI) containing wastewater.

Heavy metal ions in the contaminant water or soil often coexist with common salts at a relatively higher concentration, which brings difficulties in the removal of the heavy metals with a low concentration due to the interference and competitive effects. For example, tannery industrial wastewater contains about 80 g/L of NaCl (Lefebvre and Moletta, 2006), and the concentration of Cl^- in the groundwater of

Yuncheng basin, China, is 1686 mg/L (Li et al., 2016a). The existence of the salts highly suppresses the removal efficiency in the treatment of heavy metal ions. To this end, the adsorbents with selective ability to trap heavy metal ions are quite intriguing to researchers (Kanel et al., 2005; Rapti et al., 2016; Liu et al., 2008). For example, zero-valent iron and Fe_3O_4/HA were found to selectively adsorb Cr(VI) or other heavy metals in the real water matrix or coexisting with salt ions (Kanel et al., 2005; Liu et al., 2008). More recently, metal organic framework composites were studied to selective adsorb Cr(VI) by chemical complexation (Rapti et al., 2016). In these studies, the surface properties of adsorbents are considered to affect the selective adsorption of heavy metal ions, although further work needs to be done on the elaboration of specific mechanisms.

Biochar, as the derivative of carbon-rich residues (e.g. wood, corn straw, grass, apricot stone), has increasingly attracted researchers' attention due to its abilities in improving soil fertility, sequestering carbon, realizing the transformation of waste and adsorbing pollutants (Chen et al., 2011; Godlewska et al., 2017; Lehmann et al., 2006). Being pyrolyzed at low temperature and free of activation agents make biochar less cost, although at the expense of high surface area, as compared to activation carbon. One of the most intriguing advantages of biochars lies in the presence of plenty of functional surface groups, such as carboxyl, hydroxyl, and phenolic functional groups, which are potential to be the sites to bind heavy metal ions (Klasson et al., 2009; Sun et al., 2014; Uchimiya et al., 2011; Zhao et al., 2017).

In recent years, environmentally persistent free radicals (EPFRs) have attracted increasing attentions in respect of their adverse impacts on health (Lomnicki et al., 2008; Wang et al., 2018). EPFRs are formed during the pyrolysis of biomass in the presence of metal oxides via a mechanism of chemisorption followed by electron transfer (Lomnicki et al., 2008). They are relatively stable, and exist in the atmosphere for hours and days (Fang et al., 2014). It had been reported that semiquinone type EPFRs can induce O_2 to form $O_2^{\bullet-}$ (Khachatryan et al., 2011). Thereafter, EPFRs were used to degrade *p*-nitrophenol and activate H_2O_2 to produce •OH for the degradation of 2-chlorobiphenyl (Fang et al., 2014; Yang et al., 2016). Until now, more attentions were focused on the effects of EPFRs to generate reactive oxygen species (ROS), with the aim of degrading organic pollutants (Fang et al., 2013; Yang et al., 2016). To the best of our knowledge, no work has reported about the effect of biochar-based persistent free radicals in the treatment of heavy metals. As EPFRs can transfer electrons to oxygen, H_2O_2, and persulfate to induce Fenton reactions (Fang et al., 2013; Fang et al., 2014; Khachatryan et al., 2011; Yang et al., 2016), they can, in principle, act as reductants to react with heavy metal ions with a relatively higher redox potentials (e.g. CrO_4^{2-}), such that the reducible heavy metal ions with a less mobility can be produced and readily removed.

In this paper, environment-friendly biochars pyrolyzed from corn straw, were chosen to remove Cr(VI) in the presence of the competitive ions at a relatively higher concentration, with the aim to study the selective adsorption capacities of corn straw biochars on Cr(VI). Fourier Transform Infrared (FTIR) spectroscopy, X-ray

photoelectron spectra (XPS), X-ray absorption near edge spectra (XANES) and electron spin resonance (ESR) were applied to elucidate the selective adsorption and removal mechanisms of Cr(VI) on the biochars. ESR was used to quantify biochar-based EPFRs and their effects on the removal of Cr(VI). By introducing H_2O_2 and C_2H_5OH as the competitive scavengers, the role of EPFRs in the removal of Cr(VI) was further investigated and elucidated.

2. Materials and methods

2.1.Biochar preparation

Corn straw was selected as the precursor to prepare biochars. The precursor was crushed and sieved through a 0.25 mm mesh. Then, it was put into a stainless steel reactor (10.5 cm in height and 6.5 cm in diameter) with a lid and heated in a muffle furnace at 300°C, 500°C and 700°C for 2 h. The products were allowed to cool at room temperature, followed by washing with 1 M HCl (36%-38%, Sinopharm Chemical Reagent Co., Ltd.) and 3 M HF (40%, Sinopharm Chemical Reagent Co., Ltd.) solution to remove the ash materials. After drying in an oven at 105°C for 24 h, the biochars were lightly ground and homogenized before passing through a 210 μm sieve. The biochars pyrolyzed at 300°C, 500°C, and 700°C were labeled as C300, C500, and C700, respectively. Some biochars were further immersed into different concentrations of HNO_3 (2, 6, 10, 14 M) to activate the surface of biochars. After shaking for 48 h, the solid products were washed with deionized water until the pH was ~7, and then oven-dried at 105°C for 24 h. C500 treated by 14 M HNO_3 was referred as 14 M-C500.

2.2.Adsorption experiments

Adsorption isotherms were measured through a batch equilibrium experiment. The ratio of solid adsorbents to solution used for the adsorption experiment and selective adsorption experiment was 50 mg/20 mL. Cr(VI) solution were prepared by analytical grade $K_2Cr_2O_7$ (99.8%, Sinopharm Chemical Reagent Co., Ltd.) at different concentrations ranging from 25 to 950 mg/L, which were then mixed with 50 mg of biochars. The mixtures were shaken at room temperature (RT) for 24 h. Afterwards, the mixtures were centrifuged at 5000 rpm and filtered through 0.45 μm membrane for Cr(VI) analysis with ICP-OES (OPTIMA 8300, USA). All samples were run in triplicate.

For selective adsorption experiment, Cr(VI) at different concentration (1, 2, and 5 mg/L) was mixed with high concentrations of Cl^- (180, 1800, 3600, and 9000 mg/L). For other salt ions (NO_3^-, SO_4^{2-}, HPO_4^{2-}, F^-, $HCO_3^-$and CO_3^{2-}), 5 mg/L of each salt were mixed with 5 mg/L of Cr(VI). The other experiment procedures were the same as the adsorption isotherm experiment. All samples were run in triplicate.

In order to study the removal efficiency of Cr(VI) by the biochars pretreated with H_2O_2 and ethanol, the biochars were immersed into 25 mL of H_2O_2 or ethanol at different concentrations and shaken for 12 h. The solid products were then collected, thoroughly washed with deionized water and oven-dried for 24 h. For immersing time series experiments, the biochars were mixed with 25 mL of 40 mM H_2O_2 and 0.1 mM ethanol, respectively. All the adsorption was conducted at pH~7.

2.3.Data Analysis

The adsorption amounts of Cr(VI) on the biochars were calculated by the following equation:

$$q_e=V(C-C_e)/m \quad (1)$$

For the selective adsorption experiments, the removal efficiency, *R*%, was calculated as followed:

$$R\%=(C-C_e/\ C)\times 100\% \quad (2)$$

The adsorption isotherm models were used to describe Cr(VI) adsorption as follows:

$$q_e=K_PC_e \quad (3)$$

$$q_e=KaC_e/(1+KC_e) \quad (4)$$

$$q_e=K_FC_e^n \quad (5)$$

Here, q_e is adsorbed amount, C is initial solution concentration, C_e is equilibrium solution concentration, V is the volume of solution, and m is the mass of biochar. Equation (3), (4) and (5) represent linear model, Langmuir model, and Freundlich model, respectively. K_P is partition coefficient, K is Langmuir constant, a is Langmuir maximum capacity, K_F is Freundlich coefficient, and n is surface heterogeneity index (Hu et al., 2005; Kanel et al., 2005).

3. Results and discussion

3.1. Biochar characterization

SEM is used to characterize the morphology and surface structure of biochars. C500 and C700, pyrolyzed at a higher temperature, clearly show a tunneling structure with micropores inside. In contrast, the low temperature product, C300, has an intact structure without any tunnels and visible pores. The similarity of the isotherm curves

for C500 and C700 suggests that N_2 adsorption on the samples may follow the same pattern because of their similar surface and pore structure. The N_2 adsorption and desorption isotherm constitutes typical IV type curves with hysteresis loop of H4 for C500 and C700. As for C300, it is obvious that this gives a "S" shape which is described as type II isotherm. BET analysis reveals that the surface area of C300 is only 5.09 m^2/g, which is much lower than surface areas of C500 (241.83 m^2/g) and C700 (417.83 m^2/g) (see Table 1). Total pore volume, mesopore volume and micropore volume increase with the increasing temperature. It is found that higher temperature promotes the formation of porous structure. The micro porosity of C300, C500 and C700 increases from 0 to 46.26% and 59.83%, respectively. The ash content of corn straw is 7.35%. The biochars pyrolyze at 300 ºC, 500 ºC and 700ºC before acid treatment contain the ash contents of 10.79%, 23.27% and 26.10%, respectively. The acid treatment leads to the reduction of ash (Table 2). The content of oxygen decreases with the elevation of pyrolysis temperature, meaning the decrease of the oxygenated functional groups on the surface of biochars (de la Rosa et al., 2011). From the IR spectra of biochars, it can be seen that the intensities of both OH stretching vibration of phenolic groups (3407 cm^{-1}) and aromatic carbonyl/carboxyl C=O stretching vibration (1707 cm^{-1}) drastically reduce with the increase of pyrolysis temperature (Özçimen and Ersoy-Meriçboyu, 2010). This suggests that oxygen containing groups, such as carboxylic and hydroxyl groups, on the surface of biochars decrease as the pyrolysis temperature arising, which is coincident with the elemental analysis.

3.2. Adsorption isotherms

For all the adsorption isotherms, the adsorption amounts of Cr(VI) increase with the increase of equilibrium Cr(VI) concentrations and then reach a constant value. Different models are applied to fit the data and the obtained parameters are listed in Table 3. Langmuir isotherms can fit quite well the data for C500 and C700, with the high correlation coefficients (R^2) of 0.99 and 0.99, respectively. This indicates biochars are uniform and have a homogeneous surface distribution. The adsorption of Cr(VI) ions on the surface of biochar is monolayer. However, C300 shows the adsorption behavior different to C500 and C700, considering the slope of the adsorption isotherm. Moreover, the maximum adsorption capacity of C300 is obtained as 33.33 mg/g, as compared to 22.03 mg/g for C500 and 26.18 mg/g for C700. The different adsorption capacity may be attributed to the differing properties of each biochar resulting from functional groups and surface structure. Although the direct comparison of corn straw biochar with other adsorbents is difficult because of the different experimental conditions. The maximum adsorption capacity obtained in this study is relatively higher, as compared to oak wood biochar (3.03 mg/g, pH 2, 48 h), oak bark biochar (4.61 mg/g, pH 2, 48 h) and municipal sewage sludge biochar (7 mg/g, no pH adjustment, overnight) (Mohan et al., 2011; Chen et al., 2015). *K* is the affinity parameter which is proportional to surface area. The surface area of C700 is 1.73 times the size of C500 (Table 1), but there are no obvious difference for the maximum adsorption capacity. Combining with the elemental analysis, IR analysis and textural analysis of biochars, it can be reasonably deduced that the adsorption of

Cr(VI) on C700 is mainly controlled by physical adsorption related to the surface area of adsorbent. The surface area of C300 is 5.09 m^2/g and much smaller than the latter two biochars. The adsorption of Cr(VI) is highly related to oxygen containing groups on the biochar instead of the surface area for C300, on the basis of IR analysis, which is consistent with the previous report by that oxygen containing groups are involved in the adsorption of heavy metals (Ashkenazy et al. 1997). For C500, it is controlled by surface area and oxygen containing groups.

3.3. Adsorption of Cr(VI) in salt solution

Fig. 2a shows the removal efficiency of Cr(VI) in NaCl solution by the biochars. The selectivity can be kept for Cr(VI) coexisting with ~1000 times of NaCl. As shown in Fig. 2a, for C300 and C500 which have rich surface functional groups, only 68% and 77% of 5 mg/L Cr(VI) in the non-salt solution are removed, respectively. Therefore, the addition of NaCl facilitates the adsorption of Cr(VI). This can be attributed to the compression of the thickness of the diffuse double layer which surrounds solid and liquid phases. For C700 that has a higher surface area, the coexisting salt shows a competitive effect on the adsorption of Cr(VI). The adsorption capacity of Cr(VI) on bamboo charcoal grafted by Cu^{2+}-N-aminopropylsilane complexes also reduces with increase of ion strength (Wu et al., 2017). For the biochars prepared at different temperatures, their selective adsorption ability of Cr(VI) follows the order of C300>C500>C700. This suggests that the selective adsorption of Cr(VI) in salt solution by the biochars is probably related to the oxygen-containing groups on the surface of biochars. The biochars also show a highly selective

adsorption of Cr(VI) at even lower concentrations of 1 and 2 mg/L (see Fig. 2b). The effect of pH on the removal efficiency of Cr(VI) in NaCl solution is presented in Fig. 2c. It reveals that the removal efficiencies increase as pH decreasing. In principle, decreasing pH in solution will bring more positive charges on the surface of biochars, which favors the adsorption of Cr(VI), in view of electrostatic attraction (Wang et al., 2017).

HNO_3 treatment is an effective oxidization method to increase the surface oxygen groups of biochars, especially the content of carboxylic groups and hydroxyl groups (Li et al., 2016b). In order to amplify the effect of oxygen-containing groups on the selective adsorption of Cr(VI), the biochars are pretreated by HNO_3 with varied concentrations before used as adsorbents. C700 is chosen as an example to investigate the effect of HNO_3, since it is less positive resistance to salt relative to the other two biochars. As shown in Fig. 3a, the removal efficiencies of 5 mg/l Cr(VI) in 9000 mg/L Cl^- solution by C700 are remarkably increased after HNO_3 treatment and are proportional to the concentration of HNO_3. In micro-IR spectra, the peak intensities at 1713 cm^{-1} and 3407-3433 cm^{-1} enhance with the increase of HNO_3 concentration, which means that the contents of both hydroxyl groups and aromatic carbonyl/carboxyl groups increased after HNO_3 treatment. The previous studies also confirm that HNO_3 treatment increase oxygenated functional groups of biochars (Jin et al., 2013; Jin et al., 2018). The BET results reveal that the treatment of 10 M HNO_3 leads to the decreases of surface area, pore volume and average pore size of the biochar C700, as compared to the pristine one. This suggests that the adsorption of

Cr(VI) corresponding to the effect of textural properties of the biochar will be decreased. However, the removal efficiency of Cr(VI) by the biochar after HNO_3 treatment is actually increased. Combining with the FTIR analysis on the surface groups of the biochar before and after HNO_3 treatment, it can be deduced that oxygen-containing functional groups facilitate the removal of Cr(VI).

In order to further check the selective removal ability of biochars to other salts, the competitive adsorption of Cr(VI) is also performed in the solution with NO_3^-, SO_4^{2-}, HPO_4^{2-}, F^-, HCO_3^-, and CO_3^{2-} solution separately. Fig. 3b shows the effects of individual anions on the biochars before (C500) and after HNO_3 treatment (14 M-C500). For C500, NO_3^-, and SO_4^{2-} ions show little competition on Cr(VI) uptake. But the presence of HPO_4^{2-}, F^-, $HCO_3^-$and CO_3^{2-} obviously suppress the removal efficiency of Cr(VI), in which CO_3^{2-} shows a stronger competitor for Cr(VI). For the biochar after HNO_3 treatment (14 M-C500), it shows a remarkable improvement of selective adsorption of Cr(VI), even for the Cr(VI)/ CO_3^{2-} system.

3.4. SEM-EDAX, XPS and XANES analysis

The presence of Cr on the biochars is checked by SEM-EDAX. EDAX mappings clearly show that Cr is homogeneously distributed on the surface of biochars. In order to analyze the valent state of Cr, high resolution Cr *2p* XPS spectra are collected from three Cr(VI)-loaded biochars, C300, C500, and C700. As shown in Fig. 4, the pronounced bands appear at the binding energies of 575-580 and 585-590 eV, which are corresponding to the Cr 2*p* 3/2 and Cr 2*p* 1/2 orbitals, respectively. Specifically, Cr(VI) compound is characterized by higher binding energy of 579.0 eV-579.5 eV,

while the bands at the binding energies of 577.5 eV and 587.2 eV are assigned to Cr(III) (Choppala et al., 2016). It is clear to see that for all the three samples, the intensities of spectra are dominantly contributed from Cr(III). By quantifying the ratio of two species of chromium, the contents of Cr(VI) were obtained as 5.45% and 5.22% on the surface of C500 and C700, respectively, while Cr(III) is exclusively found on the surface of C300.

The XPS results are coincident with the measurements from XANES, as shown in Fig. 4d. The Cr *K*-edge XANES spectra of Cr on all three biochars show a small pre-edge feature of Cr(VI) at ΔE=3.0 eV, which indicates the existence of a small portion of Cr(VI) on the surface of biochars. LCF is performed for the obtained XANES spectra by using the reference Cr(III) and Cr(VI) compounds. The fitting results are shown in Fig. 4d and Table 4. For C500 and C700, the spectra consists of ~10% Cr(VI) and ~90% Cr(III), while for C300, almost all Cr(VI) on the surface of the biochar is reduced to Cr(III). The Cr *K*-edge XANES spectra, consistent with the XPS results, demonstrates that Cr(VI) adsorbed on the surface of biochars are predominantly reduced to Cr(III).

It is widely reported that Cr(VI) can be reduced to Cr(III) in acidic condition, typically at pH 2~4. But at an increasing pH, Cr(VI) is very slowly reduced to Cr(III) (Choppala et al., 2016; Dong et al., 2011; Jiang et al., 2014). It is proposed that during the reduction of Cr(VI), protons are consumed as follows:

$$HCrO_4^- + 7H^+ + 3e^- \leftrightarrow Cr^{3+} + 4H_2O \quad (6)$$

$$CrO_4^{2-} + 8H^+ + 3e^- \leftrightarrow Cr^{3+} + 4H_2O \quad (7)$$

In this sense, acidic conditions are favorable for the reduction of Cr(VI) to

Cr(III), considering that a lower pH can produce a higher redox potential of Cr(VI)/Cr(III) and thus the electrons from relatively week electron-donors by the surface groups (e.g. hydroxyl groups) of biochars will be readily donated to Cr(VI) (Mohan and Pittman, 2006). However, Cr(VI) in this case is effectively reduced to Cr(III) by the biochars at a neutral condition (The pH value is monitored as 6~7). The results suggest that a relatively stronger electron-donor is located on the surface of biochars, where EPFRs probably act as the reductants, as mentioned above.

3.5. The effect of EPFRs on the removal of Cr(VI)

EPFRs on the surface of biochars are monitored by the ESR measurements. For all the biochars, the pronounced ESR signals are observed, which confirms the existence of free radicals on the surface of sorbents (Fang et al., 2013; Fang et al., 2014; Khachatryan et al., 2011; Lomnicki et al., 2008; Yang et al., 2016). The concentration of EPFRs highly depends on the temperature and time of pyrolysis of biomass (Fang et al., 2015a). In order to investigate the effect of EPFRs on the removal of Cr(VI), EPFRs are quantitatively recorded before and after the treatment of Cr(VI). As shown in Fig. 5a, there is a very small change of EPR intensities between the biochar C300 and the one in the blank solution for 24 h. The calculated free radical concentrations, according to the integral area of the EPR peaks of C300 and C300 in water solution are 3.966×10^{18}spins/g and 3.702×10^{18}spins/g, respectively. But after the treatment of Cr(VI) (950 mg/L Cr, 24 h, RT), the free radical concentration on the biochar markedly decrease to 1.658×10^{18}spins/g. It suggests that the free radicals on the surface of biochars are consumed during the

removal of Cr(VI) in solution. Spectroscopic splitting factors (g-values) for the biochars before and after the treatment of Cr(VI) have same value of 2.004 (see Table 5), which indicates that the free radicals belong to oxygen-centered radicals of semiquinone radicals (Fang et al., 2015b). The g factor is close to the free electron g factor (2.0023) (Cui et al., 2016), indicating that EPFRs have the properties of free electron. Therefore, it is reasonable to deduce that the EPFRs on the biochars can directly donate electrons to reduce Cr(VI) into Cr(III). In this case, the redox reaction can proceed in the neutral condition. If there is no EPFR in the system, the electrons required for the reduction of Cr(VI) are possibly supplied from hydroxyl or catechol groups on the biochars (Mohan et al., 2011; Park et al., 2004). Such groups are relatively weak electron donors and thus a lower pH is needed to get a higher redox potential for reduce Cr(VI) into Cr(III) in the equations (6) and (7).

It has been reported that semiquinone-type EPFRs are found in various environmental systems, which can transfer electron to molecular oxygen to produce superoxide radical ions (Fang et al., 2015b). In this study, it is proved that oxygenated functional groups on the biochars are proved to facilitate the removal of Cr(VI). Together with the previous studies, it can be hypothesized that semiquinone-type EPFRs on the biochars directly react with chromate by transferring electron to reduce Cr(VI), accompanied by forming quinone groups on the biochars. Quinone and hydroquinone has been identified in biochar (Rogovska et al., 2017). The proposed mechanism is depicted in Fig. 5b.

In order to further verify the effect of EPFRs on the reduction and removal of Cr(VI), H_2O_2 and ethanol are used as the radical transfer or scavenger to decrease the concentration of free radicals (Kozmer et al., 2016). As shown in Fig. 6a, the ESR measurements for the biochar after the treatment of H_2O_2 and ethanol reveal a pronounced decrease of EPFRs concentration from 3.966×10^{18} to 2.695×10^{18} and 3.515×10^{18}spins/g, respectively (see Table 5). As a result, the decrease of EPFRs on the treated biochars leads to an obvious suppress of the removal efficiency of Cr(VI). It is shown in Fig. 6b-c and S5a-b, that the removal efficiency of Cr(VI) decreases with the increase of both the concentration and the treatment time of the two scavengers. It is worth noting that the maximum concentrations of H_2O_2 and ethanol used in this study are 0.6% and 0.038% of mass, respectively. Such a low concentration will, in principle, have little impact on the biochar's structure. On the other hand, it is reported that the biochars modified by 10% H_2O_2 normally have a higher percentage of oxygen-containing groups, which can increase the adsorption efficiency of heavy metals (Xue et al., 2012). The opposite result obtained in this systems further confirms the decent effect of EPFRs on the removal of Cr(VI). Similar results are also acquired by using O_2, instead of H_2O_2, to scavenge EPFRs, see the results in supporting information.

4. Conclusions

The biochars prepared from corn straw biomass show an excellent selective removal of Cr(VI) in the highly saline water. The removal efficiency of Cr(VI) increased with the increase of the oxygenated functional groups on biochars from

30.30% to 94.41%. More than 90% of Cr(VI) adsorbed on biochars were reduced to Cr(III), which could be easily removed by forming chromium hydroxide, and thereafter precipitates on the surface of adsorbents. The EPFRs on the biochars were found and proved to play a role in reducing Cr(VI). This study provides a new strategy to effectively remove heavy metal ions in highly saline solutions.

Acknowledgments

The authors thank the Beijing Synchrotron Radiation Facility (BSRF, China) for providing the beam time of 4B7A and 1W2B. The authors also acknowledge the financial support from National Key Research and Development Program of China (2016YFA0203101, 2017YFA0207204), the "One Hundred Talents Program" in Chinese Academy of Sciences.

Appendix A. Supplementary data

Supplementary data associated with this article can be found, in the online version.

References

[1]Ashkenazy, R., Gottlieb, L., Yannai, S., 1997. Characterization of acetone-washed yeast biomass functional groups involved in lead biosorption. Biotechnol. Bioeng. 55(1), 1-10.

[2]Chen, X.C., Chen, G.C., Chen, L.G., Chen, Y.X., Lehmann, J., McBride, M.B., Hay, A.G., 2011. Adsorption of copper and zinc by biochars produced from pyrolysis of hardwood and corn straw in aqueous solution. Bioresour. Technol. 102(19), 8877-8884.

[3]Chen, T., Zhou, Z., Xu, S., Wang, H., Lu, W., 2015. Adsorption behavior comparison of trivalent and hexavalent chromium on biochar derived from

municipal sludge. Bioresour. Technol. 190, 388-394.

[4]Choppala, G., Bolan, N., Kunhikrishnan, A., Bush, R., 2016. Differential effect of biochar upon reduction-induced mobility and bioavailability of arsenate and chromate. Chemosphere 144, 374-381.

[5]Cui, Y., Xu, B.W., Yang, B., Yao, H.F., Li, S.S., Hou, J.H., 2016. A novel pH neutral self-doped polymer for anode interfacial layer in efficient polymer solar cells. Macromolecules 49(21), 8126-8133.

[6]de la Rosa, J.M., Gonzalez-Perez, J.A., Gonzalez-Vila, F.J., Knicker, H., Araujo, M.F., 2011. Molecular composition of sedimentary humic acids from South West Iberian Peninsula: A multi-proxy approach. Org. Geochem. 42(7), 791-802.

[7]Dong, X.L., Ma, L.N.Q., Li, Y.C., 2011. Characteristics and mechanisms of hexavalent chromium removal by biochar from sugar beet tailing. J. Hazard. Mater. 190(1-3), 909-915.

[8]Fang, G.D., Gao, J., Dionysiou, D.D., Liu, C., Zhou, D.M., 2013. Activation of persulfate by quinones: free radical reactions and implication for the degradation of PCBs. Environ. Sci. Technol. 47(9), 4605-4611.

[9]Fang, G.D., Gao, J., Liu, C., Dionysiou, D.D., Wang, Y., Zhou, D.M., 2014. Key role of persistent free radicals in hydrogen peroxide activation by biochar: Implications to organic contaminant degradation. Environ. Sci. Technol. 48(3), 1902-1910.

[10]Fang, G.D., Liu, C., Gao, J., Dionysiou, D.D., Zhou, D.M., 2015a. Manipulation of persistent free radicals in biochar to activate persulfate for contaminant degradation. Environ. Sci. Technol. 49(9), 5645-5653.

[11] Fang, G.D., Zhu, C.Y., Dionysiou, D.D., Gao, J., Zhou, D.M., 2015b. Mechanism of hydroxyl radical generation from biochar suspensions: Implications to diethyl phthalate degradation. Bioresour. Technol. 176, 210-217.

[12]Ghosh, G., Bhattacharya, P.K., 2006. Hexavalent chromium ion removal through micellar enhanced ultrafiltration. Chem. Eng. J. 119(1), 45-53.

[13]Godlewska, P., Schmidt, H.P., Ok, Y.S., Oleszczuk, P., 2017. Biochar for composting improvement and contaminants reduction. A review. Bioresour. Technol. 246, 193-202.

[14]Hu, J., Chen, G.H., Lo, I.M.C., 2005. Removal and recovery of Cr(VI) from wastewater by maghemite nanoparticles. Water Res. 39(18), 4528-4536.

[15]Jiang, W.J., Cai, Q., Xu, W., Yang, M.W., Cai, Y., Dionysiou, D.D., O'Shea, K.E., 2014. Cr(VI) Adsorption and reduction by humic acid coated on magnetite. Environ. Sci. Technol. 48(14), 8078-8085.

[16]Jin, H., Wang, X., Gu, Z., Polin, J. 2013. Carbon materials from high ash biochar for supercapacitor and improvement of capacitance with HNO_3 surface oxidation. J. Power Sources 236, 285-292.

[17]Jin, J., Li, S., Peng, X., Liu, W., Zhang, C., Yang, Y., Han, L.F., Du, Z.W., Sun, K., Wang, X., 2018. HNO_3 modified biochars for uranium(VI) removal from aqueous solution. Bioresour. Technol. 256, 247-253.

[18]Kanel, S.R., Manning, B., Charlet, L., Choi, H., 2005. Removal of arsenic(III) from groundwater by nanoscale zero-valent iron. Environ. Sci. Technol. 39(5), 1291-1298.

[19]Khachatryan, L., Vejerano, E., Lomnicki, S., Dellinger, B., 2011. Environmentally Persistent Free Radicals (EPFRs). 1. generation of reactive oxygen species in aqueous solutions. Environ. Sci. Technol. 45(19), 8559-8566.

[20]Klasson, K.T., Wartelle, L.H., Rodgers, J.E., Lima, I.M., 2009. Copper(II) adsorption by activated carbons from pecan shells: Effect of oxygen level during activation. Ind. Crop. Prod. 30(1), 72-77.

[21]Kozmer, Z., Takacs, E., Wojnarovits, L., Alapi, T., Hernadi, K., Dombi, A., 2016. The influence of radical transfer and scavenger materials in various concentrations on the gamma radiolysis of phenol. Radiat. Phys. Chem. 124, 52-57.

[22]Lefebvre, O., Moletta, R., 2006. Treatment of organic pollution in industrial saline wastewater: A literature review. Water Res. 40(20), 3671-3682.

[23]Lehmann J., Gaunt J., Rondon M.B., 2006. Bio-char sequestration in terrestrial ecosystems- a review, Mitig. Adapt. Strateg. Glob. Change 11, 403-427.

[24]Li, C.C., Liu, T., Xu, S., Gao, X.B., Wang, Y.X., 2016a. Groundwater salinization in shallow aquifers adjacent to a low-altitude inland salt lake: a case study at Yuncheng Basin, northern China. Environ. Earth Sci. 75(5), 14.

[25]Li, H.Y., Ye, X.X., Geng, Z.G., Zhou, H.J., Guo, X.S., Zhang, Y.X., Zhao, H.J., Wang, G.H., 2016b. The influence of biochar type on long-term stabilization for Cd and Cu in contaminated paddy soils. J. Hazard. Mater. 304, 40-48.

[26] Liu, J.F., Zhao, Z.S., Jiang, G.B., 2008. Coating Fe_3O_4 magnetic nanoparticles with humic acid for high efficient removal of heavy metals in water. Environ. Sci. Technol. 42(18), 6949-6954.

[27]Lomnicki, S., Truong, H., Vejerano, E., Dellinger, B., 2008. Copper oxide-based model of persistent free radical formation on combustion-derived particulate matter. Environ. Sci. Technol. 42(13), 4982-4988.

[28]Mohan, D., Pittman, C.U., 2006. Activated carbons and low cost adsorbents for remediation of tri- and hexavalent chromium from water. J. Hazard. Mater. 137(2), 762-811.

[29]Mohan, D., Rajput, S., Singh, V.K., Steele, P.H., Pittman, C.U., 2011. Modeling and evaluation of chromium remediation from water using low cost bio-char, a green adsorbent. J. Hazard. Mater. 188(1-3), 319-333.

[30]Mohan, D., Singh, K.P., Singh, V.K., 2006. Trivalent chromium removal from wastewater using low cost activated carbon derived from agricultural waste material and activated carbon fabric cloth. J. Hazard. Mater. 135(1-3), 280-295.

[31]Özçimen, D., Ersoy-Meriçboyu, A., 2010. Characterization of biochar and bio-oil samples obtained from carbonation of various biomass materials. Renew. Energ. 35, 1319-1324.

[32]Park, D., Yun, Y.S., Park, J.M., 2004. Reduction of hexavalent chromium with the brown seaweed Ecklonki biomass. Environ. Sci. Technol. 38(18), 4860-4864.

[33]Rapti, S., Pournara, A., Sarma, D., Papadas, I.T., Armatas, G.S., Tsipis, A.C., Lazarides, T., Kanatzidis, M.G., Manos, M.J., 2016. Selective capture of hexavalent chromium from an anion-exchange column of metal organic resin-alginic acid composite. Chem. Sci. **7**(3), 2427-2436.

[34]Rogovska, N., Laird, D., Leandro, L., Aller, D., 2017. Biochar effect on severity of soybean root disease caused by Fusarium virguliforme. Plant Soil 413 (1-2), 111-126.

[35]Sun, J.K., Lian, F., Liu, Z.Q., Zhu, L.Y., Song, Z.G., 2014. Biochars derived from various crop straws: Characterization and Cd(II) removal potential. Ecotox. Environ. Safe. 106, 226-231.

[36]Tiravanti, G., Petruzzelli, G., Passino, R., 1997. Pretreatment of tannery wastewaters by an ion exchange process for Cr(III) removal and recovery. Water Sci. Technol. 36(2-3), 197-207.

[37]Uchimiya, M., Chang, S., Klasson, K.T., 2011. Screening biochars for heavy metal retention in soil: Role of oxygen functional groups. J. Hazar. Mater. 190(1-3), 432-441.

[38]Wang, G.F., Wang, S., Sun, W., Sun, Z.M., Zheng, S.L., 2017. Synthesis of a novel illite@carbon nanocomposite adsorbent for removal of Cr(VI) from wastewater. J. Environ. Sci. 57, 62-71.

[39]Wang, P., Pan, B., Li, H., Huang, Y., Dong, X.D., Ai, F., Liu, L.Y., Wu, M., Xing, B.S., 2018. The overlooked occurrence of environmentally persistent free radicals in an area with low-rank coal burning, Xuanwei, China. Environ. Sci. Technol. 52, 52, 1054-1061.

[40]Wu, Y.H., Ming, Z., Yang, S.X., Fan, Y., Fang, P., Sha, H.T., Cha, L.G., 2017. Adsorption of hexavalent chromium onto Bamboo Charcoal grafted by Cu^{2+}-N-aminopropylsilane complexes: Optimization, kinetic, and isotherm studies. J. Ind. Eng. Chem. 46, 222-233.

[41]Xue, Y.W., Gao, B., Yao, Y., Inyang, M., Zhang, M., Zimmerman, A.R., Ro, K.S., 2012. Hydrogen peroxide modification enhances the ability of biochar (hydrochar) produced from hydrothermal carbonization of peanut hull to remove aqueous heavy metals: Batch and column tests. Chem. Eng. J. 200, 673-680.

[42]Yang, J., Pan, B., Li, H., Liao, S.H., Zhang, D., Wu, M., Xing, B.S., 2016. Degradation of p-nitrophenol on biochars: Role of persistent free radicals. Environ. Sci. Technol. 50(2), 694-700.

[43]Yu, X., Jiang, Y.M., Huang, H.Y., Shi, J.J., Wu, K.J., Zhang, P.Y., Lv, J.G., Li, H.L., He, H., Liu, P., Li, X.K., 2016. Simultaneous aerobic denitrification and Cr(VI) reduction by *Pseudomonas brassicacearum* LZ-4 in wastewater. Bioresour. Technol. 221, 121-129.

[44]Zhao, N., Zhao, C.F., Lv, Y.Z., Zhang, W.F., Du, Y.G., Hao, Z.P., Zhang, J., 2017. Adsorption and coadsorption mechanisms of Cr(VI) and organic contaminants on H_3PO_4 treated biochar. Chemosphere 186, 422-429.

Figure captions

Fig.1. Isotherm data for the adsorption of Cr(VI) by the biochars. (Lines represent Langmuir fitting and the bars are standard errors.)

Fig.2. (a) Removal efficiency of Cr(VI) by the biochars in the binary solution with 5 mg/L Cr(VI) and different concentrations of Cl^- at pH 7. (b) Removal efficiency of Cr(VI) by biochars in binary solution systems with low concentrations of Cr(VI) and low concentrations of Cl^-. (c) Removal efficiency of Cr(VI) by C300 biochar at different pH values in the binary solution (The bars are standard errors).

Fig.3. (a) Removal efficiency of 5 mg/L Cr(VI) coexisting with 9000 mg/L Cl^- by C700 pretreated with different concentrations of HNO_3. (b) Removal efficiency of Cr(VI) coexisting with different salt ions by C500 and 14 M-C500. (The bars are standard errors.)

Fig.4. XPS analysis of Cr in the Cr(VI) loaded biochar prepared at 300°C (a), 500°C (b) and 700°C (c). Cr *K*-edge XANES spectra for the biochars (C300, C500, and C700) after adsorption, and the reference spectra of $K_2Cr_2O_7$, $Cr(OH)_3$ and $CrCl_3$ for fitting. The circle dots stand for experimental spectra and the red curves are fitting data (d).

Fig.5. (a) ESR spectra of C300 in the blank solution, and before and after the adsorption of Cr(VI). (b) Proposed mechanism for the reduction of Cr(VI) by EPFRs on the biochars.

Fig.6. (a) ESR spectra of C300 pretreated with 200 mM H_2O_2 and 6.5 mM C_2H_5OH. (b-c) Removal efficiency of Cr(VI) by C300 pretreated with different concentrations of H_2O_2 (b) and C_2H_5OH (c). (The bars are standard errors.)

Table 1

The BET surface area and pore morphology of biochars.

Samples	Surface area (m^2/g)	Total pore volume (cm^3/g)	Mesopore volume (cm^3/g)	Micropore volume (cm^3/g)[a]	Average pore size (nm)
C300	5.09	0.0036	0.000	0.000	35.16
C500	241.83	0.1472	0.035	0.068	3.76
C700	417.83	0.2391	0.088	0.143	4.63
10M-C700	291.72	0.1707	0.047	0.088	4.11

[a]Micropore volume is obtained by the cumulative pore volume of the micropores that calculated by t-plot. Mesopore volume is obtained by the cumulative pore volume of the mesopores that calculated by Barret-Joyner-Halenda (BJH).

Table 2

Elemental composition (on a dry mass basis), atomic ratio and ash of biochars.

Samples	C (%)	H (%)	N (%)	O (%)	H/C	O/C	C/N	(O+N)/C	Ash (%)
C300	61.67	5.41	1.88	31.04	1.05	0.43	38.27	0.46	0.44
C500	72.49	2.97	2.09	20.75	0.49	0.25	40.46	0.27	1.70
C700	83.76	1.50	1.76	10.42	0.21	0.11	55.52	0.12	2.56

Table 3

Parameters of different isotherm equations for Cr(VI) adsorption

Sample	Linear		Langmuir			Freundlich		
	$q_e=K_PC_e$		$q_e=KaC_e/(1+KC_e)$			$q_e=K_FC_e^n$		
	K_P (L/g)	R^2	K (L/g)	a (mg/g)	R^2	K_F (mg/g (L/mg) ^{n})	n	R^2
C300	0.036±0.001[a]	0.45	0.004±0.000	33.33±3.035	0.97	0.439±0.030	0.640±0.017	0.94
C500	0.029±0.001	-0.44	0.012±0.003	22.03±2.072	0.99	1.853±0.149	0.379±0.016	0.92
C700	0.035±0.001	-0.65	0.013±0.001	26.18±1.433	0.99	2.868±0.124	0.327±0.012	0.95

[a] Values are mean ± standard errors.

Table 4

Cr(VI) and Cr(III) contents determined by LCF fitting method.

	C300	C500	C700
Cr(VI)	0	0.099	0.094
Cr(III)	1	0.901	0.906
R-factor	0.0009	0.0002	0.0007

Table 5

ESR parameters for the biochars before and after interacting with Cr(VI)

Samples	EPFRs concentration (spins/g × 10^{18})	Line width (Gauss)	Spectroscopic splitting factor (g)
C300	3.966	4.786	2.004
C300-H_2O	3.702	4.860	2.004
C300-Cr(VI)	1.658	6.032	2.004
H_2O_2-C300	2.695	4.908	2.004
C_2H_5OH-C300	3.515	4.762	2.004

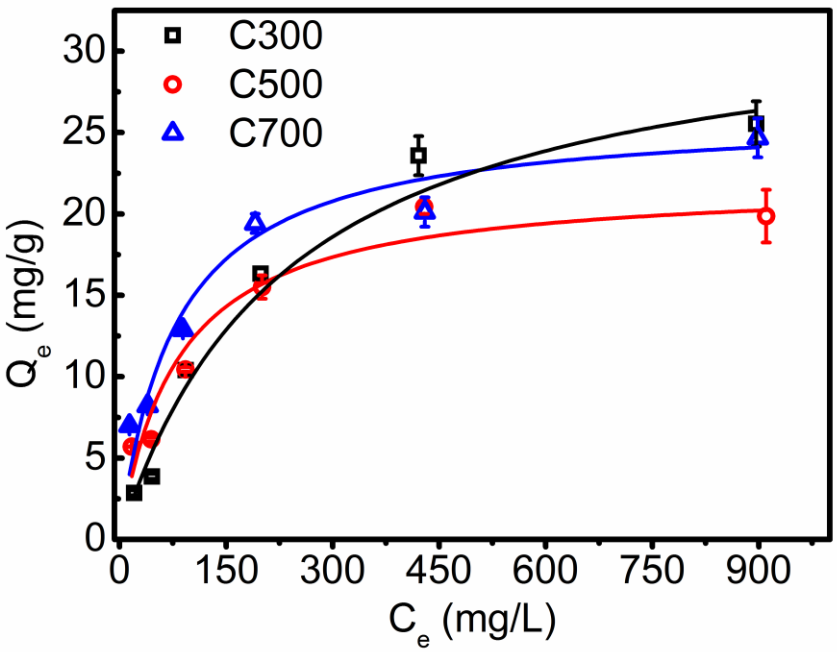
C300
C500
C700
30
25
20
15
10
5
0
Q_e (mg/g)
0
150
300
450
600
750
900
C_e (mg/L)

Fig.1.

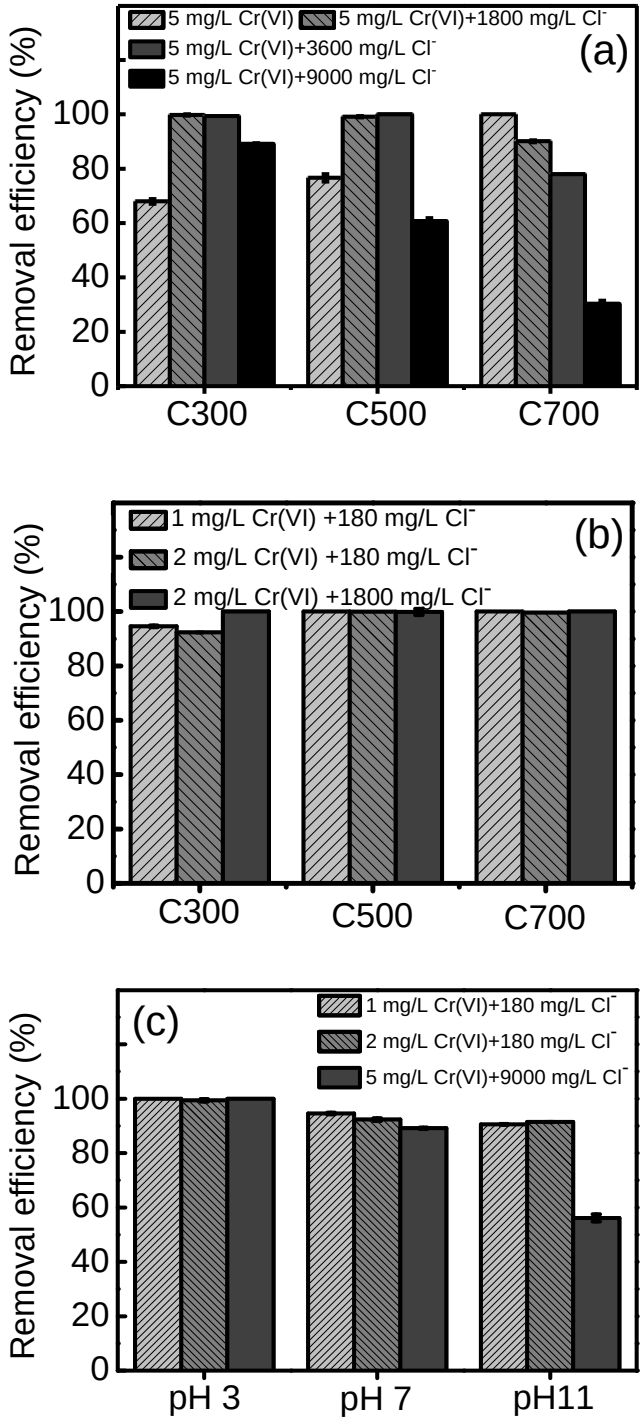
5 mg/L Cr(VI)
5 mg/L Cr(VI)+1800 mg/L Cl-
5 mg/L Cr(VI)+3600 mg/L Cl-
5 mg/L Cr(VI)+9000 mg/L Cl-
(a)
Removal efficiency (%)
0
20
40
60
80
100
C300
C500
C700
1 mg/L Cr(VI) +180 mg/L Cl-
2 mg/L Cr(VI) +180 mg/L Cl-
2 mg/L Cr(VI) +1800 mg/L Cl-
(b)
Removal efficiency (%)
0
20
40
60
80
100
C300
C500
C700
(c)
1 mg/L Cr(VI)+180 mg/L Cl-
2 mg/L Cr(VI)+180 mg/L Cl-
5 mg/L Cr(VI)+9000 mg/L Cl-
Removal efficiency (%)
0
20
40
60
80
100
pH 3
pH 7
pH11

Fig.2.

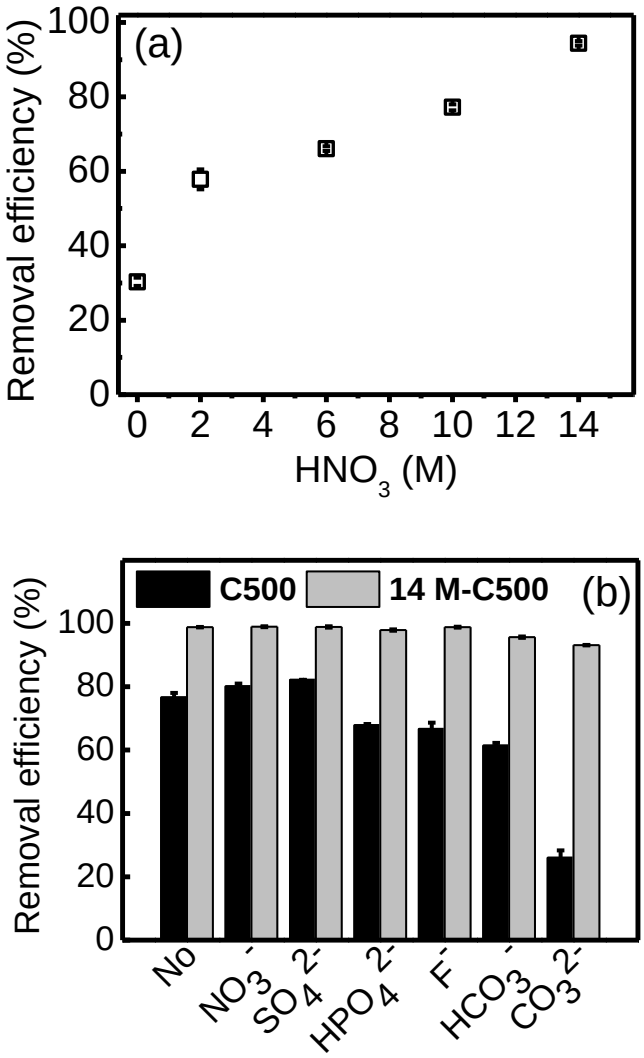
(a)
Removal efficiency (%)
100
80
60
40
20
0
0
2
4
6
8
10
12
14
HNO3 (M)
(b)
C500
14 M-C500
Removal efficiency (%)
100
80
60
40
20
0
No
NO3-
SO4 2-
HPO4 2-
F-
HCO3-
CO3 2-

Fig.3.

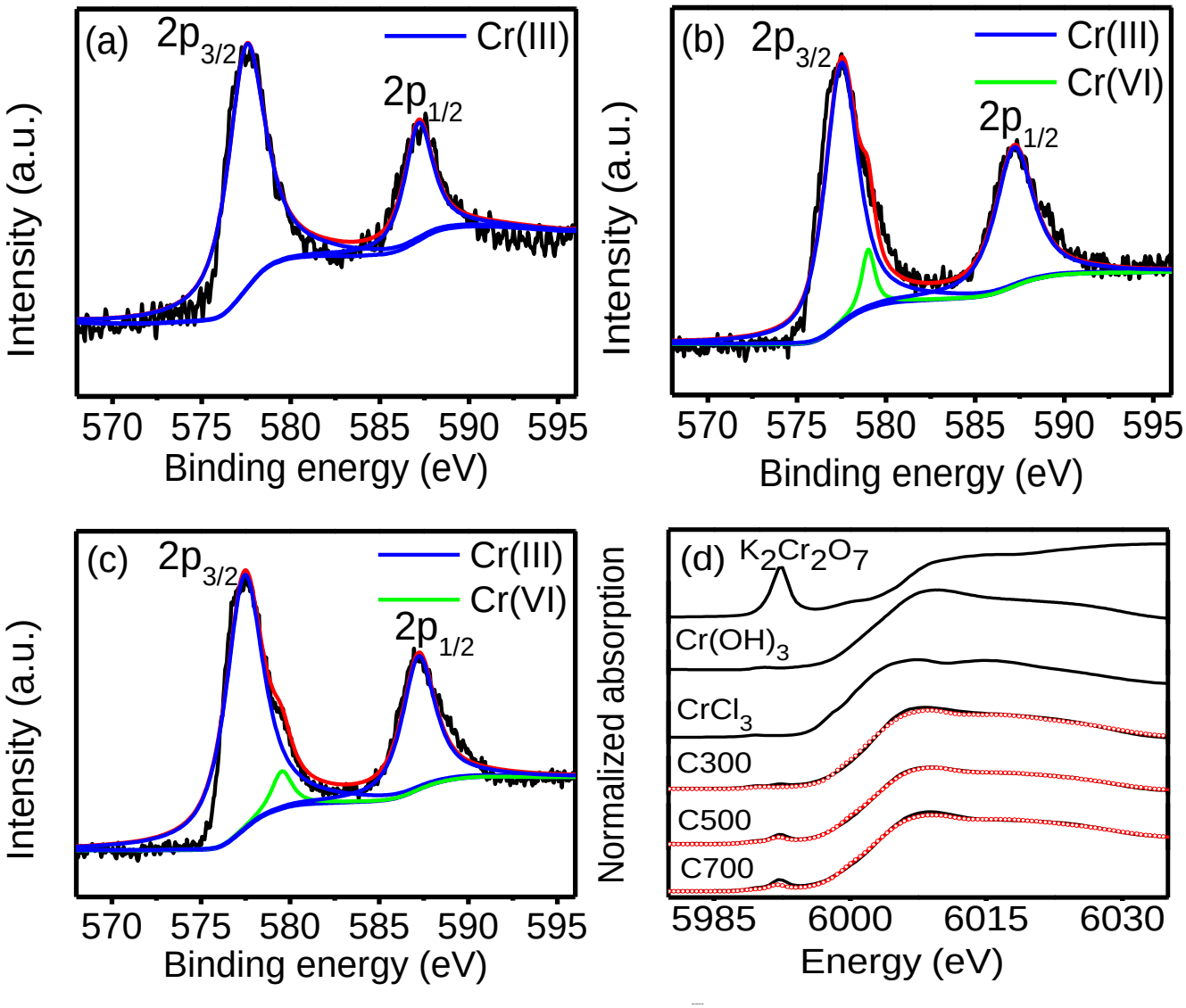
(a) 2p3/2
Cr(III)
2p1/2
Intensity (a.u.)
570 575 580 585 590 595
Binding energy (eV)
(b) 2p3/2
Cr(III)
Cr(VI)
2p1/2
Intensity (a.u.)
570 575 580 585 590 595
Binding energy (eV)
(c) 2p3/2
Cr(III)
Cr(VI)
2p1/2
Intensity (a.u.)
570 575 580 585 590 595
Binding energy (eV)
(d) K2Cr2O7
Cr(OH)3
CrCl3
C300
C500
C700
Normalized absorption
5985 6000 6015 6030
Energy (eV)

Fig.4.

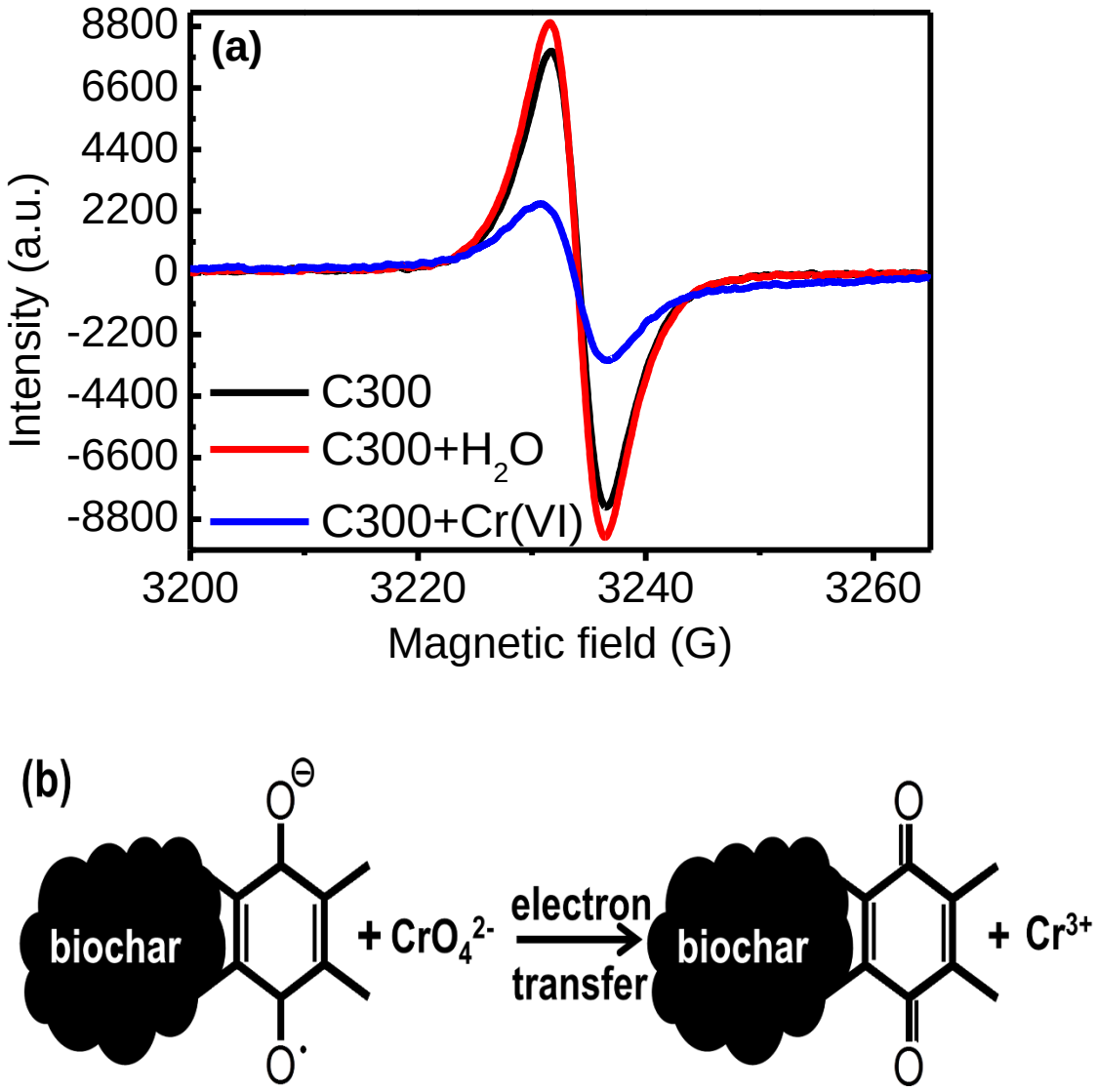
(a)
8800
6600
4400
2200
0
-2200
-4400
-6600
-8800
Intensity (a.u.)
C300
C300+H2O
C300+Cr(VI)
3200
3220
3240
3260
Magnetic field (G)
(b)
biochar
+ CrO4 2-
electron
transfer
biochar
+ Cr3+

Fig.5.

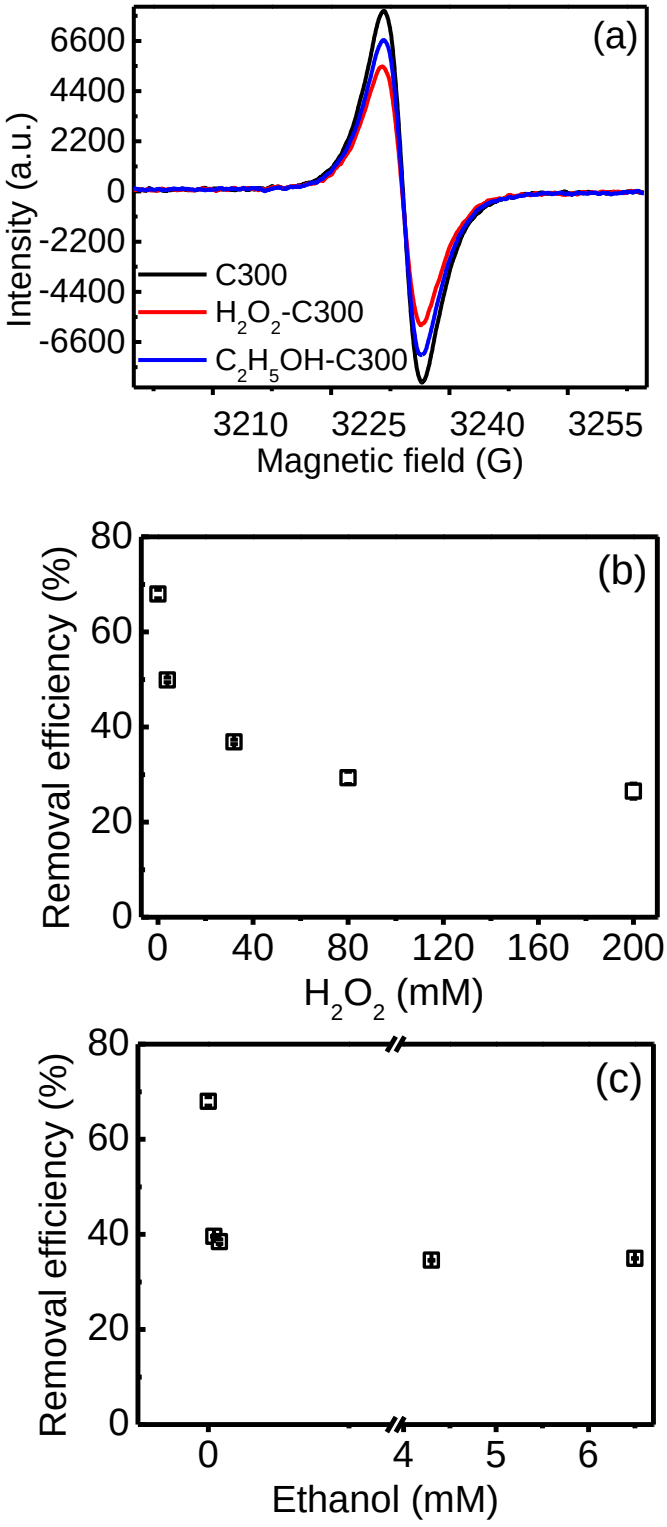
(a)
Intensity (a.u.)
6600
4400
2200
0
-2200
-4400
-6600
C300
H2O2-C300
C2H5OH-C300
3210
3225
3240
3255
Magnetic field (G)
(b)
Removal efficiency (%)
80
60
40
20
0
0
40
80
120
160
200
H2O2 (mM)
(c)
Removal efficiency (%)
80
60
40
20
0
0
4
5
6
Ethanol (mM)

Fig.6.